Epilepsia
Official Journal of the International League Against Epilepsy

Topographic principles of cortical FLAIR signal in temporal lobe epilepsy

Journal:	*Epilepsia*
Manuscript ID	EPI-01003-2017.R1
Manuscript Type:	Full length original research paper
Date Submitted by the Author:	25-Dec-2017
Complete List of Authors:	Adler, Sophie; Montreal Neurological Institute and Hospital, McGill University , Neuroimaging of Epilepsy Laboratory Hong, Seok-Jun; Montreal Neurological Institute and Hospital, McGill University , McConnell Brain Imaging Centre Liu, Min; Montreal Neurological Institute and Hospital, McGill University , McConnell Brain Imaging Centre Baldeweg, Torsten; UCL Institute of Child Health, Developmental Neuroscience Programme Cross, J.; Great Ormond Street Hospital, University College London, Department of Clinical & Experimental Epilepsy Bernasconi, Andrea; Montreal Neurological Institute and Hospital, McGill University , McConnell brain Imaging Centre Bernhardt, Boris; Montreal Neurological Institute and Hospital, McGill University , McConnell Brain Imaging Centre Bernasconi, Neda; Montreal Neurological Institute and Hospital, McGill University , McConnell Brain Imaging Centre
Key Words:	temporal lobe epilepsy, MRI, hippocampus, covariance analysis

TOPOGRAPHIC PRINCIPLES OF CORTICAL FLAIR SIGNAL IN TEMPORAL LOBE EPILEPSY

Sophie Adler[1,2], Seok-Jun Hong[1], Min Liu[1], Torsten Baldeweg[2], J. Helen Cross[2], Andrea Bernasconi[1], Boris C. Bernhardt[1,3*], Neda Bernasconi[1*]

1) NeuroImaging of Epilepsy Laboratory, McConnell Brain Imaging Center, Montreal Neurological Institute and Hospital, McGill University, Montreal, QC, Canada; 2) Developmental Neurosciences, UCL Great Ormond Street Institute of Child Health, University College London, London, UK; 3) Multimodal Imaging and Connectome Analysis Laboratory, Montreal Neurological Institute and Hospital, McGill University, Montreal, QC, Canada

* Authors contributed equally to the work

RUNNING TITLE: FLAIR mapping in TLE

DOCUMENT SPECIFICATIONS
19 pages
3 figures, 1 table, 1 supplementary figure
2799 words (295/574/670 words in summary/introduction/discussion)
40 references

Keywords: temporal lobe epilepsy, MRI, hippocampus, covariance analysis

CORRESPONDING AUTHOR
Neda Bernasconi, MD PhD
Montreal Neurological Institute (WB-322)
3801 University Street
Montreal, Quebec, Canada H3A 2B4
Telephone: (514) 398-3044
E-mail: neda@bic.mni.mcgill.ca

SUMMARY

OBJECTIVE. In drug-resistant temporal lobe epilepsy (TLE), relative to the large number of whole-brain morphological studies, neocortical T2 changes have not been systematically investigated. The aim of this study was to assess the anatomical principles that govern the distribution of neocortical T2-weighted fluid attenuation inversion recovery (FLAIR) signal intensity and uncover its topographic principles.

METHODS. Using a surface-based sampling scheme, we mapped neocortical FLAIR intensity of 61 TLE patients relative to 38 healthy controls imaged at 3T. To address topographic principles of the susceptibility to FLAIR signal changes in TLE, we assessed associations with normative data on tissue composition using two complementary approaches. First, we evaluated whether the degree of TLE-related FLAIR intensity changes differed across cytoarchitectonic classes as defined by Von Economo-Koskinas taxonomy. Secondly, as a proxy to map regions with similar intra-cortical composition, we carried out a FLAIR intensity covariance paradigm in controls by seeding systematically from all cortical regions, and identified those networks that were the best spatial predictors of the between-group FLAIR changes.

RESULTS. Increased intensities were observed in bilateral limbic and paralimbic cortices (hippocampus, parahippocampus, cingulate, temporopolar, insular, orbitofrontal). Effect sizes were highest in periallocortical limbic and insular classes as defined by the Von Economo-Koskinas cytoarchitectonic taxonomy. Furthermore, systematic FLAIR intensity covariance analysis in healthy controls revealed that intensity similarity patterns characteristic of limbic cortices, most notably the hippocampus, served as sensitive predictors for the topography of FLAIR hypersignal in patients. FLAIR intensity findings were robust against correction for morphological confounds. Patients with a history of febrile convulsions showed more marked signal changes in parahippocampal and retrosplenial cortices, known to be strongly

connected to the hippocampus.

SIGNIFICANCE. FLAIR intensity mapping and covariance analysis provide a model of TLE grey matter pathology based on shared vulnerability of periallocortical and limbic cortices.

Keywords: temporal lobe epilepsy, MRI, hippocampus, covariance analysis

INTRODUCTION

Temporal lobe epilepsy (TLE) is the most common drug-resistant epilepsy in adults. Magnetic resonance imaging (MRI) analyses, specifically volumetry on T1-weighted images, have been instrumental for *in vivo* identification of neuronal loss associated with hippocampal sclerosis [1], the hallmark lesion in TLE [2]. Furthermore, morphometric assessments have revealed that changes in TLE are rarely limited to the mesiotemporal structures, but found across multiple neocortical regions, supporting system-level compromise [3]. Contrary to the hippocampus [4], however, the relation between neuronal loss and measures of neocortical morphology, including cortical thickness and estimates of grey matter density [5], has not been clearly established. Arguably, changes in cortical geometry likely reflect combinations of biological events rather than specific tissue properties, limiting the biological precision of inferences that can be drawn from observations of cortical thinning in TLE.

Beside morphometry, T2 contrasts such as T2 relaxometry and FLAIR are commonly used for detection of hippocampal pathology. T2 signal hyperintensity is a sensitive marker of hippocampal sclerosis even in cases with normal hippocampal volume [6]. Combined MRI and histological analyses have shown positive associations between hippocampal T2 hyperintensity and astrogliosis [7; 8], a characteristic feature of hippocampal sclerosis beside neuronal loss. Noteworthy, animal research and analysis of postsurgical tissue has shown a role for astrocytes in hyperexcitability and seizures [9].

Relative to the large number of whole-brain morphological studies, neocortical T2 changes have not been systematically studied. A single study, restricted to patients with left TLE, used voxel-based T2 mapping [10]. While this study suggested subtle anomalies beyond the hippocampus involving the temporal lobes, voxel-based approaches may have limited sensitivity to detect cortical anomalies, as across-subject variability in sulcation challenges

measurement correspondence [11]. Moreover, voxel-wise isotropic smoothing (commonly used to improve correspondence between individuals) may reduce specificity for intracortical changes, and inflate partial volume effects. Circumventing these limitations, surface-based based algorithms currently represent a state-of-the-art approach to anatomical analysis. In relation to intensity, we have recently shown that surface-based mapping of hippocampal T2 intensity lateralizes the seizure focus in patients with no radiologically-visible anomalies [12; 13], suggesting increased yield for the detection of pathology.

Notwithstanding benefits of surface-based mapping to reveal the extent of neocortical pathology, this procedure does not *per se* provide explanations on factors governing regional susceptibility to observed anomalies. In TLE, a key determinant may be the cytoarchitectonic markup of a given region, with limbic areas showing different cellular composition and connectivity profiles to the neocortex. Observational studies in healthy adults have shown that variations in T2 signal intensity across the cortex may, in part, reflect differences in architectonic organization [14], with limbic and paralimbic allocortices displaying higher T2 intensities than six-layered isocortical regions [15].

In this study, we performed the first surface-based mapping of cortical T2-FLAIR signal in patients with drug-resistant TLE comparing them to healthy controls. To address the topographic principles that drive the susceptibility to FLAIR signal changes in TLE, we assessed associations with normative data on intra-cortical tissue composition using two complementary approaches. First, we evaluated whether the degree of TLE-related FLAIR intensity changes differed across cytoarchitectonic classes as defined in the seminal *post-mortem* work by Von Economo [16]. Secondly, as a proxy to map regions with similar intra-cortical composition, we carried out a FLAIR intensity covariance paradigm in controls by seeding systematically from all cortical regions, and identified those networks that were the best spatial predictors of the between-group FLAIR changes. Finally, we evaluated the

relationship between cortical FLAIR and clinical variables.

MATERIALS AND METHODS

Subjects

We studied 61 consecutive patients with unilateral pharmaco-resistant TLE (31 LTLE, mean±SD age=34±9 years, range=18–53 years, 11 males; 30 RTLE, 34±9 years, 20-52 years, 15 males) and 38 age- and sex-matched healthy controls (30±7 years, 20-53 years, 21 males) investigated at the Montreal Neurological Institute and Hospital. Demographic and clinical data were obtained through interviews with patients and their relatives (see **TABLE**). TLE diagnosis and lateralization of the seizure focus were determined by a comprehensive evaluation, including a detailed history and neurological examination, the review of medical records, scalp video-EEG recordings, as well as MRI assessment. Volumetry [17] and shape modeling [18] revealed ipsilateral atrophy in all patients. No patient had a mass lesion (malformations of cortical development, tumors, or vascular malformations), traumatic brain injury, or a history of encephalitis.

The comprehensive investigation recommended surgery for all patients. At the time of study, 43 had undergone a selective amygdalo-hippocampectomy. Histological analysis of the resected specimen [2] revealed neuronal cell loss and gliosis in CA1 and CA4 subfields in 17 (ILAE HS Type-1), neuronal loss predominantly in CA1 in 6 (ILAE HS Type-2), neuronal loss predominantly in CA4 in 5 (ILAE HS Type-3) and gliosis only without detectable neuronal loss in 15. Post-operative seizure outcome was determined according to Engel's modified classification [19] after a follow-up time of 52±21 months (range: 14-88 months). Among the operated patients, 30 (70%) had Class-I outcome, 7 (16%) Class-II, 5 (12%) Class-III, and 1 (2%) Class-IV. We observed comparable rates of seizure-free patients across HS subtypes [Type-1: 15/17 (88%), Type-2: 4/6 (66%), Type-3: 5/5 (100%), $\chi 2=2.57$, $P > 0.1$], while rates were lower in patients with isolated gliosis [6/15 (40%), $\chi 2=9.21$, $P =$

0.002]. Among the 18 non-operated patients, nine await surgery and nine delayed it for personal reasons.

The Ethics Committee of the Montreal Neurological Institute and Hospital approved the study and written informed consent was obtained from all participants.

Imaging

MRI data were obtained on a 3T Siemens TimTrio (Siemens Healthcare, Erlangen, Germany), using a 32-channel head coil. We acquired 3D T1-weighted (T1w) magnetization-prepared rapid gradient echo images (MPRAGE; TR=2300 ms, TE=2.98 ms, TI=900 ms, FA=9°, FOV=256×256 mm^2, matrix=256×256, 176 sagittal slices, 1×1×1 mm^3 voxels; 5.30 min) as well as submillimetric 3D FLAIR (Turbo spin echo; TR=5000 ms, TE=389 ms, TI=1800 ms, FA=variable, FOV=207×207 mm^2, matrix=230×230, 173 sagittal slices, 0.9×0.9×0.9 mm^3 voxels; 7.37 min).

Image processing

T1w and FLAIR images underwent correction for intensity non-uniformity [20] and intensity normalization. T1w images were linearly registered to the MNI152 symmetric template. FLAIR images were linearly registered to T1-weighted images, and subsequently registered to MNI152 space based on the previously estimated registration. T1w data were classified into white matter (WM), grey matter (GM), and cerebro-spinal fluid (CSF). Using the Constrained Laplacian Anatomic Segmentation using Proximity (CLASP) algorithm [21], we generated models of the inner (GM-WM) and outer (GM-CSF) cortical surfaces and measured cortical thickness across 81,924 corresponding surface points (*henceforth*, vertices). Surfaces were visually verified and corrected if necessary. Cortical thickness was calculated as the straight line distance between corresponding points on the inner and outer surface [22], and surface-smoothed using a diffusion kernel with 20mm full-width-at-half-maximum.

To examine intracortical signal intensity [23], we created three equidistant surfaces positioned between the GM-CSF and GM-WM at 25%, 50%, and 75% cortical thickness guided by a straight line providing vertex correspondence across these surfaces. We normalized voxel-wise FLAIR intensity measures by the mode of the FLAIR intensity histogram and the intensity at the GM-WM boundary. Normalized intensities were mapped to the nearest vertex of each intra-cortical surface. Notably, we did not sample intensity on the outermost (*i.e.,* GM-CSF) surface to avoid CSF contamination. At remaining surfaces, we corrected intensities for residual CSF partial volume effect as in a previous study. Data were blurred with a surface-based 20mm Gaussian diffusion kernel. Finally, we averaged normalized intensities across the three intra-cortical surfaces to create average cortical T1w and FLAIR signal intensities per vertex.

Statistical Analysis

Analyses were performed using SurfStat (http://www.math.mcgill.ca/keith/surfstat/) for Matlab. Patients were analyzed relative to the epileptogenic hemisphere (*i.e.,* ipsi- and contralateral to the focus). To control for hemispheric asymmetry, we z-normalized intensity and cortical thickness at each vertex with respect to the corresponding distribution in healthy controls (*i.e.,* each patient's right/left feature was expressed as a z-score with respect to right/left values in controls).

a) Mapping FLAIR signal intensity. We compared cortical FLAIR signal intensity between patients and controls using vertex-wise Student's t-tests. In clusters of findings, we computed the average effect size using the Cohen's d metric. To evaluate robustness, similar to our previous work [22], we carried out a bootstrap based approach in which patient and control groups were randomly resampled with replacement for 1,000 times and compared against each other.

b) Relation to cortical morphology. We compared cortical thickness between patients and controls, and assessed overlaps between cortical thinning and FLAIR changes. To fully rule out effects of morphology, invariant to statistical thresholds, we repeated the FLAIR group comparisons after statistically controlling for vertex-wise cortical thickness.

c) Relationship to post-mortem cytoarchitectonic classes. We mapped the cytoarchitectonic atlas of Von Economo-Koskinas to cortical surface models, by adapting a previously published approach [24]. Subsequently, we manually assigned cytoarchitectonic class labels to each atlas parcel (Class I: granular cortex, primary motor; II and III: association cortex; IV: dysgranular cortex, primary and secondary sensory; V: agranular cortex, primary sensory; VI: limbic cortex, allocortex; VII, insular cortex), similar to a recent work [25].

d) Relationship to cortical intensity covariance networks. We used automated anatomical labeling (AAL) to parcellate the neocortex into 78 cortical regions [26]. We furthermore added the hippocampus as an additional region-of-interest (see Subjects section). We carried out a FLAIR intensity covariance analysis of each region-of-interest to the entire neocortex in our healthy controls, which provides a spatial map representing a network whose intensity characteristics correlate strongest with the seed region. We then correlated each of these networks with the map of between group FLAIR alterations across the cortical surface, an approach resembling 'network epicentre' mapping [27].

e) Relation to clinical variables. Using surface-wide linear models, we assessed effects of history of febrile convulsions, age at seizure onset, and duration of epilepsy on FLAIR signal intensity. In patients who had undergone surgery, we repeated group comparisons based of histological grade, *i.e.,* separately analyzing patients with hippocampal sclerosis and isolated gliosis and assessed the relation to post-operative seizure outcome.

f) Correction for multiple comparisons. Surface-based findings were corrected using random field theory for non-isotropic images [28], controlling for family-wise error (FWE) below

$P_{FWE}<0.05$.

RESULTS

Surface-based mapping of FLAIR

Compared to controls, TLE patients presented with bilateral hippocampal FLAIR signal intensity increases (ipsilateral: t=3.99, p<0.001; contralateral: t=2.25, p=0.03), with larger effect sizes ipsilateral to the seizure focus (Cohen's d=0.83 ipsilateral; d=0.47 contralateral). Patients also displayed bilateral symmetric neocortical FLAIR hyperintensity in limbic and paralimbic cortices (*i.e.,* parahippocampus, cingulate, temporopolar, insular, orbitofrontal cortices), as well as in the dorsolateral prefrontal cortex, superior parietal lobule, and the precuneus (**FIGURE 1A**; $P_{FWE}<0.05$). In these regions, we observed moderate-to-high effect sizes (d=0.68-0.89). Assessing separately left and right TLE patients confirmed FLAIR increases across all clusters ($P_{FWE}<0.05$). Bootstrap analysis indicated that the topography of anomalies was reproducible in 70-100% of simulations. Comparing only TLE patients with histologically-confirmed hippocampal sclerosis (*i.e.,* HS Type 1, 2 and 3) to controls resulted in a topography of FLAIR hyperintensity similar to the whole-group findings (**Supplementary FIGURE**).

Relationship to cortical thinning

Comparing TLE patients to controls, we observed areas of cortical thinning in bilateral frontal, temporal and central cortices (**FIGURE 1B**; $P_{FWE}<0.05$), in line with our previous findings [22]. Importantly, patterns of significant cortical thinning overlapped only minimally with those displaying FLAIR hyperintensity (Dice index=9.1%), suggesting feature complementarity. Indeed, repeating the between-group FLAIR comparisons after regressing out vertex-wise cortical thickness revealed virtually identical results (**FIGURE 1C**; $P_{FWE}<0.05$).

Relationship to cytoarchitectonic classes and intensity covariance networks

Assessing FLAIR changes across the cytoarchitectural classes based on the Von Economo-Koskinas *post mortem* grading, we observed highest effects (d>0.4, P<0.05 Bonferroni corrected) in allocortical limbic (Class VI) and insular cortices (Class VII; **FIGURE 2A**), followed by lower effects in the association cortex (Class II; d=0.3; P<0.05 Bonferroni corrected).

Systematic intensity covariance analysis across neocortical and hippocampal seed regions provided networks that were used as spatial 'predictors' of the between-group FLAIR difference map (see Figure 1). The best 'predictor' was the network centered on the hippocampal seed, yielding the highest vertex-wise correlation with the between-group t-statistical map (**FIGURE 2B**, r=0.27, P_{FWE}<0.001**)**, followed by networks centered on parahippocampal and anterior cingulate cortex. The hippocampal FLAIR intensity covariance network encompassed cingulate, entorhinal, posterior parahippocampal, retrosplenial, and insular cortices, as well as dorsolateral prefrontal regions. Notably, the relationship between hippocampal covariance and FLAIR between-group differences remained unchanged after regressing out geodesic distance from the ipsilateral hippocampus, computed using an approach invariant to mesh configuration, indicating that findings related to topological and not physical proximity (r=0.28, P_{FWE}<0.0001).

Relation to clinical variables

After correction for multiple comparisons, we found no association between cortical FLAIR and age at seizure onset, duration of epilepsy, post-surgical seizure freedom, or histological hippocampal sclerosis grades (P_{FWE}>0.2). On the other hand, patients with a history of febrile convulsions exhibited a pattern of FLAIR increases resembling the patients *vs.* controls differences, with significant clusters in ipsilateral parahippocampal and retrosplenial

cortices (P_{FWE}<0.05, **FIGURE 3**).

DISCUSSION

Using a surface-based paradigm that samples signal intensity within the cortical mantle, we mapped the distribution of neocortical FLAIR signal anomalies in TLE patients relative to controls. We observed a pattern of hyperintensity primarily in bilateral limbic and paralimbic regions, including hippocampal, parahippocampal, insular, cingulate and dorsolateral prefrontal cortices, as well as the orbitofrontal cortex. The topography of FLAIR anomalies was highly similar in left and right TLE patients, reproducible across histological subtypes, and replicable across thousands of bootstrap resampling experiments, supporting consistency.

Contrary to FLAIR changes, patterns of cortical thinning were primarily observed in frontal and lateral temporal cortices corroborating earlier work [22; 29]. Divergence in the anatomical distribution of morphological markers and those related to intensity as in this work suggests that these imaging markers reflect different aspects of TLE pathology [10; 13]. In agreement with our current findings, we also recently showed that changes in T1 relaxation time, a quantitative marker putative marker of myelin, do not overlap with morphological anomalies [30]. While cortical thinning may relate to grey matter atrophy, possibly secondary to excitotoxic effects of seizure spread through thalamo-cortical pathways [31], FLAIR hypersignal possibly reflects specific vulnerability of limbic and paralimbic cortices to TLE pathology. Support for this finding came from our analysis of regions-of-interest stratified by cytoarchitecture, which indicated higher effect sizes particularly in insular and cingulate regions. Furthermore, cross-reference of TLE-specific hyperintensity with regionally unbiased *in vivo* intensity matching in controls, suggested that regions with similar intensity covariations as the hippocampus may be particularly susceptible. These findings collectively

support a shared susceptibility model based on cytoarchitecture. Indeed, while the identified network spanned across both temporo-limbic as well as prefrontal regions belonging to diverse cytoarchitectonic classes, the largest proportion fell into the periallocortex, at transition between the three-layered allocortical limbic areas (such as the hippocampus) and the six-layered isocortex. In the healthy human brain, limbic and paralimbic cortices appear hypertintense compared to the isocortex [15]. Notably, in primates, some of these regions display high glial cell density [32], which could contribute to the signal profile we observed. Further support for FLAIR hyperintensity being driven by glial cell composition comes from our findings in the prefrontal region, a non-limbic granular cortex. This region positioned between the primary motor cortex and frontal eye fields has been shown to display high glial cell counts at the expense of low neuronal density [33]. It is thus plausible that differing cellular composition and laminar architecture, drive both FLAIR signal covariance and susceptibility to FLAIR-detectable pathology.

Correlative studies have shown a close association between hippocampal T2 hyperintensity and gliosis [8]. As our patients underwent a selective amygdalo-hippocampectomy, specimens were restricted to the mesiotemporal, precluding a histopathological verification of neocortical group-level findings. While we cannot exclude possible contributions of iron and myelin to T2-weighted signal [34], our data may be compatible with an extensive gliotic process. This hypothesis is supported by histopathological studies reporting neocortical grey matter gliosis in areas similar to those we report, including the frontal pole and orbitofrontal regions [35]. Long considered a bystander of neuronal damage, evidence from animal models and clinical studies suggest a link between astrogliosis, neuronal excitability, and seizure genesis [9]. Interestingly, clinical correlation analysis indicated an association between cortical FLAIR hyperintensity (particularly the ipsilateral parahippocampal cortex) and a history of febrile convulsions. This finding

provides a broader perspective on studies documenting visually appreciable hippocampal T2 hyperintensity following febrile seizures in children who eventually develop epilepsy [36; 37]. While acute, peri-ictal T2 changes may reflect a different pathophysiological process, likely cytotoxic edema [38], the chronic FLAIR changes we demonstrate may be secondary to chronic glial cell activation. Indeed, studies in animal models of status epilepticus indicate that chronic glial cell activation extends beyond the hippocampus into other limbic cortices, including the parahippocampal region [39]; importantly, glial alterations may even precede neuronal loss [40].

In conclusion, by highlighting periallocortical transition zones and limbic cortices, FLAIR intensity mapping and covariance analysis provide a support for a susceptibility model of TLE grey matter pathology based on cytoarchitecture.

ACKNOWLEDGMENTS

This work was supported by the Canadian Institutes of Health Research (CIHR MOP-57840 and MOP-123520). SA received funding from the Rosetrees Trust and Charlotte and Yule Bogue Research Fellowships. BCB acknowledges salary support by the Fonds de la Recherche du Quebec - Santé. None of the authors has any conflict of interest to disclose. We confirm that we have read the Journal's position on issues involved in ethical publication and affirm that this report is consistent with those guidelines.

KEY POINT BOX

- Patients with drug-resistant TLE demonstrate neocortical FLAIR hyperintensities in bilateral limbic and paralimbic cortices.
- FLAIR intensity covariance of the hippocampus in controls predicts the topography of hyperintensities in TLE.

- FLAIR mapping and covariance analysis provide a model of TLE grey matter pathology based on shared cytoarchitectural vulnerability.

REFERENCES

1. Duncan JS, Winston GP, Koepp MJ, et al. Brain imaging in the assessment for epilepsy surgery. *Lancet Neurol* 2016;15:420-433.
2. Blumcke I, Thom M, Aronica E, et al. International consensus classification of hippocampal sclerosis in temporal lobe epilepsy: a Task Force report from the ILAE Commission on Diagnostic Methods. *Epilepsia* 2013;54:1315-1329.
3. Bernhardt BC, Hong S, Bernasconi A, et al. Imaging structural and functional brain networks in temporal lobe epilepsy. *Frontiers in human neuroscience* 2013;7:624.
4. Cascino GD, Jack CR, Jr., Parisi JE, et al. Magnetic resonance imaging-based volume studies in temporal lobe epilepsy: pathological correlations. *Ann Neurol* 1991;30:31-36.
5. Eriksson SH, Thom M, Symms MR, et al. Cortical neuronal loss and hippocampal sclerosis are not detected by voxel-based morphometry in individual epilepsy surgery patients. *Hum Brain Mapp* 2009;30:3351-3360.
6. Bernasconi A, Bernasconi N, Caramanos Z, et al. T2 relaxometry can lateralize mesial temporal lobe epilepsy in patients with normal MRI. *Neuroimage* 2000;12:739-746.
7. Kosior RK, Sharkey R, Frayne R, et al. Voxel-based relaxometry for cases of an unresolved epilepsy diagnosis. *Epilepsy Res* 2012;99:46-54.
8. Goubran M, Bernhardt BC, Cantor-Rivera D, et al. In vivo MRI signatures of hippocampal subfield pathology in intractable epilepsy. *Human Brain Mappping* 2015;HBM-15-0662.
9. Devinsky O, Vezzani A, Najjar S, et al. Glia and epilepsy: excitability and inflammation. *Trends Neurosci* 2013;36:174-184.
10. Pell GS, Briellmann RS, Pardoe H, et al. Composite voxel-based analysis of volume and T2 relaxometry in temporal lobe epilepsy. *Neuroimage* 2008;39:1151-1161.
11. Bookstein FL. "Voxel-based morphometry" should not be used with imperfectly registered images. *Neuroimage* 2001;14:1454-1462.
12. Kim H, Bernhardt BC, Kulaga-Yoskovitz J, et al. Multivariate hippocampal subfield analysis of local MRI intensity and volume: application to temporal lobe epilepsy. *Med Image Comput Comput Assist Interv* 2014;17:170-178.
13. Bernhardt BC, Bernasconi A, Liu M, et al. The spectrum of structural and functional imaging abnormalities in temporal lobe epilepsy. *Ann Neurol* 2016;80:142-153.
14. Georgiades CS, Itoh R, Golay X, et al. MR imaging of the human brain at 1.5 T: regional variations in transverse relaxation rates in the cerebral cortex. *AJNR Am J Neuroradiol* 2001;22:1732-1737.
15. Hirai T, Korogi Y, Yoshizumi K, et al. Limbic lobe of the human brain: evaluation with turbo fluid-attenuated inversion-recovery MR imaging. *Radiology* 2000;215:470-475.
16. Von Economo C, Koskinas GN. Die Cytoarchitektonik der Hirnrinde des erwachsenen Menschen. Springer: Wien and Berlin; 1925.
17. Caldairou B, Bernhardt BC, Kulaga-Yoskovitz J, et al. A Surface Patch-Based Segmentation Method for Hippocampal Subfields. In Ourselin S, Joskowicz L, Sabuncu MR, et al. (Eds) Medical Image Computing and Computer-Assisted Intervention – MICCAI 2016: 19th International Conference, Athens, Greece, October 17-21, 2016, Proceedings, Part II, Springer International Publishing: Cham; 2016:379-387.
18. Kim H, Mansi T, Bernasconi A, et al. Vertex-wise shape analysis of the hippocampus: disentangling positional differences from volume changes. *Med Image Comput Comput Assist Interv* 2011;14:352-359.
19. Engel J, Jr., Van Ness PC, Rasmussen T, et al. Outcome with respect to epileptic seizures. In Engel J, Jr. (Ed) Surgical treatment of the epilepsies, Raven: New York; 1993:609-621.
20. Sled JG, Zijdenbos AP, Evans AC. A nonparametric method for automatic correction of intensity nonuniformity in MRI data. *IEEE Trans Med Imaging* 1998;17:87-97.
21. Kim JS, Singh V, Lee JK, et al. Automated 3-D extraction and evaluation of the inner and outer cortical surfaces using a Laplacian map and partial volume effect classification. *Neuroimage* 2005;27:210-221.
22. Bernhardt BC, Bernasconi N, Concha L, et al. Cortical thickness analysis in temporal lobe epilepsy: reproducibility and relation to outcome. *Neurology* 2010;74:1776-1784.

23. Hong SJ, Bernhardt BC, Caldairou B, et al. Multimodal MRI profiling of focal cortical dysplasia type II. *Neurology* 2017;88:734-742.
24. Scholtens LH, de Reus MA, van den Heuvel MP. Linking contemporary high resolution magnetic resonance imaging to the von Economo legacy: A study on the comparison of MRI cortical thickness and histological measurements of cortical structure. *Hum Brain Mapp* 2015;36:3038-3046.
25. Vertes PE, Rittman T, Whitaker KJ, et al. Gene transcription profiles associated with inter-modular hubs and connection distance in human functional magnetic resonance imaging networks. *Philos Trans R Soc Lond B Biol Sci* 2016;371.
26. Tzourio-Mazoyer N, Landeau B, Papathanassiou D, et al. Automated anatomical labeling of activations in SPM using a macroscopic anatomical parcellation of the MNI MRI single-subject brain. *Neuroimage* 2002;15:273-289.
27. Zhou J, Gennatas ED, Kramer JH, et al. Predicting regional neurodegeneration from the healthy brain functional connectome. *Neuron* 2012;73:1216-1227.
28. Worsley KJ, Andermann M, Koulis T, et al. Detecting changes in nonisotropic images. *Hum.Brain Mapp.* 1999;8:98-101.
29. McDonald CR, Hagler DJ, Jr., Ahmadi ME, et al. Regional neocortical thinning in mesial temporal lobe epilepsy. *Epilepsia* 2008;49:794-803.
30. Bernhardt BC, Fadaie F, Vos de Wael R, et al. Preferential susceptibility of limbic cortices to microstructural damage in temporal lobe epilepsy: A quantitative T1 mapping study. *Neuroimage* 2017.
31. Bernhardt BC, Bernasconi N, Kim H, et al. Mapping thalamocortical network pathology in temporal lobe epilepsy. *Neurology* 2012;78:129-136.
32. Collins CE, Airey DC, Young NA, et al. Neuron densities vary across and within cortical areas in primates. *Proc Natl Acad Sci U S A* 2010;107:15927-15932.
33. Zhou J, Golay X, van Zijl PC, et al. Inverse T(2) contrast at 1.5 Tesla between gray matter and white matter in the occipital lobe of normal adult human brain. *Magn Reson Med* 2001;46:401-406.
34. Eriksson SH, Free SL, Thom M, et al. Correlation of quantitative MRI and neuropathology in epilepsy surgical resection specimens--T2 correlates with neuronal tissue in gray matter. *Neuroimage* 2007;37:48-55.
35. Blanc F, Martinian L, Liagkouras I, et al. Investigation of widespread neocortical pathology associated with hippocampal sclerosis in epilepsy: a postmortem study. *Epilepsia* 2011;52:10-21.
36. Lewis DV, Shinnar S, Hesdorffer DC, et al. Hippocampal sclerosis after febrile status epilepticus: the FEBSTAT study. *Ann Neurol* 2014;75:178-185.
37. Provenzale JM, Barboriak DP, VanLandingham K, et al. Hippocampal MRI signal hyperintensity after febrile status epilepticus is predictive of subsequent mesial temporal sclerosis. *AJR Am J Roentgenol* 2008;190:976-983.
38. Scott RC, Gadian DG, King MD, et al. Magnetic resonance imaging findings within 5 days of status epilepticus in childhood. *Brain* 2002;125:1951-1959.
39. Ravizza T, Gagliardi B, Noe F, et al. Innate and adaptive immunity during epileptogenesis and spontaneous seizures: evidence from experimental models and human temporal lobe epilepsy. *Neurobiol Dis* 2008;29:142-160.
40. Kang TC, Kim DS, Kwak SE, et al. Epileptogenic roles of astroglial death and regeneration in the dentate gyrus of experimental temporal lobe epilepsy. *GLIA* 2006;54:258-271.

TABLE. Demographic and clinical information

	AGE	MEN	ONSET	DURATION	FC	SURGERY	HS	ENGEL I
LTLE (n=31)	34 ± 9	11	18 ± 10	16 ± 10	7	19	12	13 (68%)
RTLE (n=30)	34 ± 9	15	14 ± 9	20 ± 11	12	24	16	17 (71%)
Controls (n=38)	30 ± 7	21	n/a	n/a	n/a	n/a	n/a	n/a

Age, age at seizure onset, and duration of epilepsy are presented in years mean±SD. *FC:* febrile convulsions; *HS*: hippocampal sclerosis on histopathology (remaining patients had gliosis only); *ENGEL I:* seizure free (Engel I) postsurgical outcome.

LEGENDS FOR FIGURES

FIGURE 1. Surface-based mapping of neocortical FLAIR intensity and thickness.

Group differences between patients with temporal lobe epilepsy (TLE) and controls in: **A)** neocortical FLAIR signal intensity, **B)** cortical thickness and **C)** neocortical FLAIR signal intensity after regressing out cortical thickness at each surface point **(C)**. Findings have been adjusted for multiple comparisons using random field theory for non-isotropic images and thresholded at $P_{FWE}<0.05$. Blue scale indicates decreases and red scale increases. Results of the reproducibility analysis mapping the probability of observing FLAIR hyperintensity in patients *vs.* controls across 1,000 random group comparisons are shown in the insert in **A**.

FIGURE 2. Relationship to cytoarchitectonic classes and intensity covariance.

A) Comparison in FLAIR signal intensity between TLE and healthy controls (NC) across different cytoarchitectonic classes (I-VII). Stars indicate a significant between-group differences following Bonferroni-correction. **B)** Systematic intensity covariance analysis across all cortical regions revealed that the map cantered on the hippocampus (*left*) provided the highest correlation with the between-group FLAIR intensity map. The scatter plot on the *right* shows surface-wide correlation between these networks and the t-statistic of the TLE *vs.* controls group difference in FLAIR signal.

FIGURE 3. Relationship between FLAIR signal intensity and febrile convulsions.

Maps shows FLAIR signal intensity increases in patients with history of febrile convulsions relative to those without. Significant clusters, corrected for multiple comparisons using random field theory at $P_{FWE}<0.05$ are outlined in black.

SUPPLEMENTARY FIGURE. Surface-based mapping of neocortical FLAIR intensity in patients with histologically-confirmed HS.

Group differences between patients with histological confirmation of HS (Type 1, 2, 3) and controls. Significant clusters, corrected for multiple comparisons using random field theory at $P_{FWE}<0.05$ are outlined in black.

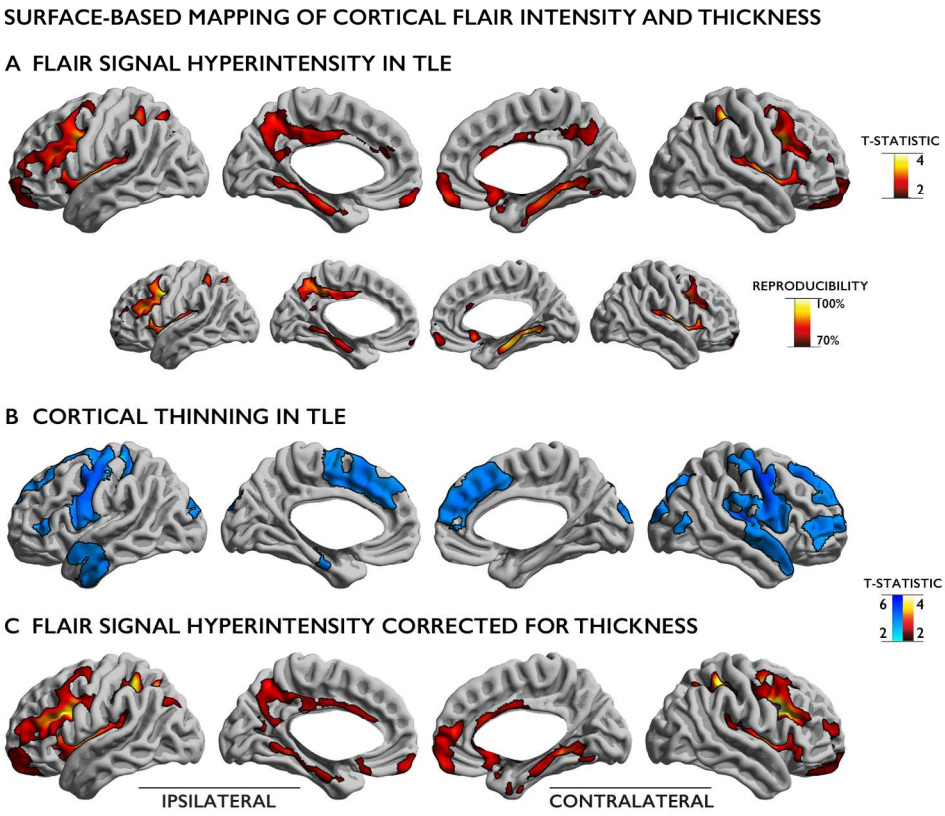

Figure 1. Surface-based mapping of neocortical FLAIR intensity and thickness. Group differences between patients with temporal lobe epilepsy (TLE) and controls in: A) neocortical FLAIR signal intensity, B) cortical thickness and C) neocortical FLAIR signal intensity after regressing out cortical thickness at each surface point (C). Findings have been adjusted for multiple comparisons using random field theory for non-isotropic images and thresholded at PFWE<0.05. Blue scale indicates decreases and red scale increases. Results of the reproducibility analysis mapping the probability of observing FLAIR hyperintensity in patients vs. controls across 1,000 random group comparisons are shown in the insert in A.

170x142mm (300 x 300 DPI)

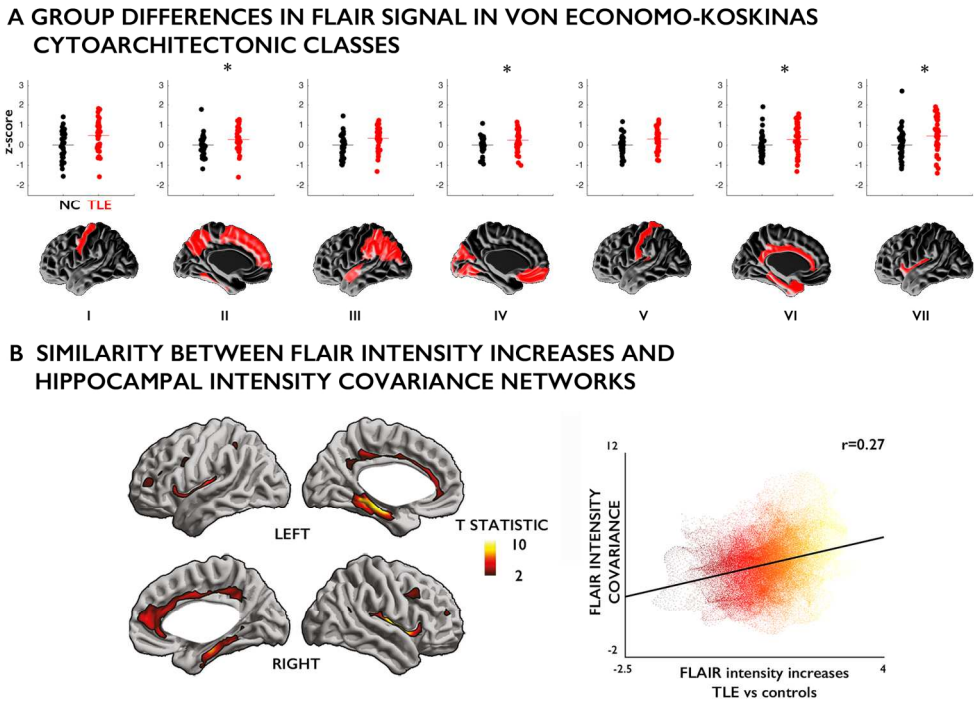

Figure 2. Relationship to cytoarchitectonic classes and intensity covariance.
A) Comparison in FLAIR signal intensity between TLE and healthy controls (NC) across different cytoarchitectonic classes (I-VII). Stars indicate a significant between-group differences following Bonferroni-correction. B) Systematic intensity covariance analysis across all cortical regions revealed that the map cantered on the hippocampus (left) provided the highest correlation with the between-group FLAIR intensity map. The scatter plot on the right shows surface-wide correlation between these networks and the t-statistic of the TLE vs. controls group difference in FLAIR signal.

152x108mm (300 x 300 DPI)

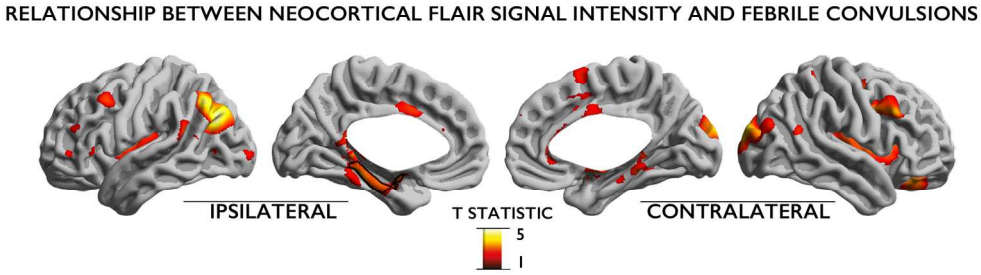

Figure 3. Relationship between FLAIR signal intensity and febrile convulsions.
Maps shows FLAIR signal intensity increases in patients with history of febrile convulsions relative to those without. Significant clusters, corrected for multiple comparisons using random field theory at PFWE<0.05 are outlined in black.

170x54mm (300 x 300 DPI)